Published in final edited form as:
Science. 2013 January 11; 339(6116): 186–189. doi:10.1126/science.1230262.

Bio-inspired Polymer Composite Actuator and Generator Driven by Water Gradients

Mingming Ma[1], **Liang Guo**[1], **Daniel G. Anderson**[1,2], and **Robert Langer**[1,2,*]

[1]David H. Koch Institute for Integrative Cancer Research, Massachusetts Institute of Technology, Cambridge, MA 02139

[2]Harvard-MIT Division of Health Sciences and Technology, and Department of Chemical Engineering, Massachusetts Institute of Technology, Cambridge, MA 02139

Abstract

Here we describe the development of a water-responsive polymer film; combining both a rigid matrix (polypyrrole) and a dynamic network (polyol-borate), strong and flexible polymer films were developed that can exchange water with the environment to induce film expansion and contraction, resulting in rapid and continuous locomotion. The film actuator can generate contractile stress up to 27 MPa, lift objects 380 times heavier than itself, and transport cargo 10 times heavier than itself. We have assembled a generator by associating this actuator with a piezoelectric element. Driven by water gradients, this generator outputs alternating electricity at ~0.3 Hz, with a peak voltage of ~1.0 V. The electrical energy is stored in capacitors that could power micro- and nano-electronic devices.

Polymeric materials that reversibly change shape, size or mechanical properties in response to external stimuli have attracted considerable interest due to their potential applications as actuators for biomedical and mechanical purposes (1). Based on their energy sources for actuation, responsive polymeric materials can be divided into three classes: electro-active polymers (2, 3); light or thermal responsive elastomers (4-9); and pH or solvent responsive gels (10-14). Many organisms use water-sorption-induced swelling for actuation (15). Several types of water-responsive hydrogels have been developed for actuator fabrication (10), but they exhibit slower response, lower stress generation and marginal stability in comparison to animal muscle fibers.

Polypyrrole (PPy) is an electro-active polymer with many desirable properties that could allow it to act as an artificial muscle (16, 17). PPy can also absorb water and change its shape, which is the basis for driving motion in a rotary actuator (18). However, existing PPy rotary actuators only weakly output mechanical force or power, in contrast to PPy-based electro-actuators (16, 18). Inspired by the network structure of animal dermis, in which rigid collagen fibers reinforce an elastic network of elastin microfibrils to form a sturdy and flexible material (19), we hypothesized that the composite of a soft water-responsive gel within a rigid polymer matrix would yield a better water-responsive actuator. We made a dynamic polymer composite of rigid PPy imbedded with a flexible, inter-penetrating polyol-borate network (20) that would be responsive to water sorption and desorption (Fig. 1A). The dynamic polyol-borate network formed within the PPy matrix also serves as a macromolecular counter ion for PPy. The polyol-borate network is sensitive to water due to hydrolysis and reforming of the borate ester crosslinking hub upon water sorption and desorption, which changes the mechanical properties of the composite (Fig. 1A).

*Correspondence to: Robert Langer, rlanger@mit.edu.

Intermolecular hydrogen bonding between the polyol-borate network and PPy also modulates intermolecular packing of the polymer composite to alter mechanical properties in response to water. Therefore, the polymer composite exhibits fast, reversible and dramatic mechanical deformation and recovery in response to environmental moisture, visually reminiscent of “fast twitch” muscle activity.

The free-standing composite polymer film was synthesized by electro-polymerization of pyrrole in the presence of a polyol-borate complex. The polyol was pentaerythritol ethoxylate (PEE), a four-armed ethylene glycol oligomer (MW ~800), which can coordinate with boron (III) species to form a dynamic polymer network as indicated by peak shifts in ^{11}B NMR spectra (20) and increased viscosity (21) (Fig. S1, S2). We hypothesized that the anionic PEE-borate complex could be electrically attracted to the cathode and trapped in the growing PPy matrix as macromolecular counter ions. We attempted to reduce the PPy matrix and export small counter ions by applying a negative electrical potential on the PEE-PPy film for 1 hour in an electrolytic solution (22). The treated PEE-PPy film showed minimal change in weight, conductivity and mechanical properties, which suggested that the counter ion is a polymeric entity and cannot be electrically transported out of the PPy matrix (22). In contrast, when this reduction-resistant PEE-PPy film was soaked in 90 °C water for 1 hour, its weight, conductivity and mechanical properties significantly decreased (Fig. S3, Table S1). PEE and boric acid were identified in the soaked water sample by NMR and IR (Fig. S4, S5). The average amount of PEE in the initial PEE-PPy film was ~12% by weight. The leached PEE and boric acid components indicated hydrolysis of the polymeric counter anion, suggestive of the water-responsive nature of the PEE-borate network (Fig. 1A) (20).

Monitored by a Quartz Crystal Microbalance with a humidity module, the PEE-PPy film rapidly absorbed up to 10% of water by weight from humid air. The film's weight change synchronized with the humidity change (Fig. 1B), indicating the film's instant response to water vapor. To probe the polymer's chemical structure change in response to water, a PEE-PPy film was immersed in D_2O for 10 s, then taken out and examined by ATR-IR. After D_2O-exposure, three IR peaks related to O-H or N-H bending disappeared and three new peaks appeared (Fig. S6, Table S2). The peak shifting was due to the hydrogen-deuterium exchange of active protons in OH and NH. The isotopic ratio (v_H/v_D) of the three peaks was smaller than the theoretical value ($v_H/v_D = 1.37$) for free O-H or N-H bonds, suggesting that these active protons were involved in hydrogen bonding (23). When this PEE-PPy film was left in ambient air (RH ~20%), the deuterium-peaks quickly shifted back to corresponding hydrogen-peaks within 4 min (Fig. 1C) without contacting any liquid water. This fast hydrogen-deuterium exchange demonstrated that the PEE-PPy film was continuously and rapidly “breathing” water from the air, which should manifest in a fast and reversible response to environmental water concentration changes. The film was also characterized by Raman spectroscopy, conductivity measurements and mechanical analysis (see supporting online material (SOM) for details), which showed a combination of moderate conductivity (30 S/cm), high tensile strength (115 MPa) and good flexibility (elongation-at-break 23%). The film also showed good stability while exposed to air and ambient humidity for six months (Fig. 1D, Fig. S7).

The PEE-PPy film spontaneously and continuously flipped and navigated over a moist nonwoven paper (Movie S1). Film motility required the water gradient, rather than just water: in a closed chamber saturated by water vapor, the PEE-PPy film folded into a roll and remained static. One locomotive cycle of the film was generally comprised of five stages (Fig. 2A, I to V). As a PEE-PPy film contacted the moist substrate, the bottom face absorbed more water than the top face, which caused asymmetric swelling and film curling away from the substrate (I). Thus, the film-substrate contact area decreased and the film's gravity center rose, which led to mechanical instability (II) and eventually caused the buckled film to

topple over (III). Asymmetric water sorption was repeated at the film-substrate interface, which cooperated with water release from the raised part of the film to generate horizontal movement (IV). Finally, most of the contact area curled up and the film fell back to the substrate with a new face down (V) to start a new cycle (I). During the flipping process (stage I-V), both faces of the film were equilibrating with water in the substrate and in the lower humidity air above. Thus, the water gradient between substrate and air was reflected in the asymmetric film deformation that drove the film locomotion with the cooperation of film gravity and friction with substrate. Analysis of the frequency of film flipping motion as a function of the saturated water vapor pressure P_s (proportional to water evaporation rate, see Equation S1) at each substrate temperature indicated a roughly linear correlation (Fig. 2B), suggesting that the film locomotion could be regulated by controlling the water evaporation rate. If the air close to the substrate was water-saturated, the PEE-PPy film would fold into a roll (VI), which possessed high elastic energy of 21-76 J/kg and could partially release the energy in a sudden and quick leap (Fig. 2A energy diagram, Movie S2, Equation S2, S3).

Water gradients were most effective in driving PEE-PPy film locomotion. Volatile polar organic solvents (e.g. alcohols, ketones, esters) also caused PEE-PPy film to swell and buckle, but translational motion was significantly weaker or unable to be completed. This can be explained by the interpenetrating polymer structure (PEE-borate network and its hydrogen-bond interaction with polypyrrole matrix) being more sensitive to water than to other organic solvents (20). We also found that PPy films without an interpenetrating PEE-borate network (18) exhibited marginal film buckling on a moist substrate with no translational motion, in contrast to a PEE-PPy film that navigated on the same substrate. The different behaviors could be attributed to the observation that water sorption had a bigger softening effect on a PEE-PPy film than on a PPy film (Fig. S8). While dry PPy and PEE-PPy films had similar tensile moduli of ~ 2.3 GPa, the moist PEE-PPy was much softer than moist PPy (young's modulus 0.65 GPa vs 1.65 GPa, Table S1). This difference could also be explained by the interpenetrating polymer structure being broken/weaken upon water sorption and recovered upon water desorption (Fig. 1A). The cooperative switching of the PEE-PPy film between the two states with different physical properties (swelling/soft vs shrinking/stiff) likely contributed to its rapid locomotion output. In addition, we also found that a larger PEE-PPy film (9 cm × 9 cm, Fig. S9) performed fast locomotion at a similar frequency as a smaller one (2 cm × 4 cm) (Movie S3), suggesting that this water-gradient-driven actuator is potentially scalable.

The contractile force and stress generated in a PEE-PPy film actuator was measured on a mechanical analyzer. A 25-mg PEE-PPy film covered by a moist paper was clamped and preloaded with 0.05 N to keep the film tight and straight. When the film was uncovered, a contractile force of up to 14 N was generated due to the film's shrinking and stiffening caused by water desorption (Fig. 3A). The maximum stress was 27 MPa, which was about 80 times higher than that of mammalian skeletal muscle (~0.35 MPa) (17) and comparable to the maximum stress electrochemically generated in other PPy-based actuators (22-34 MPa) (24, 25). When the film was again covered by a moist paper, the contractile force and stress decreased to zero as a result of the water-induced film swelling and softening. The expansion/contraction cycle could be repeated hundreds of times. One full expansion/contraction cycle needed ~5 min at room temperature and 20% RH, possibly due to slow water diffusion in the film (18). This does not conflict with the film's fast locomotion since the locomotion only needs activation forces in the mN level, which can be generated within 0.1 s in the film upon water sorption or desorption. The load-dependent stroke was measured by preloading the moist actuator up to 21 MPa. Upon water desorption, the actuator contracted under a constant load and the linear relation between stroke and load (Fig. 3B) indicated that the actuator worked in its elastic range. The maximum work during

contraction was ~73 J/kg achieved at 9-15 MPa loading, which matched the maximum elastic potential energy (76 J/kg) stored in a film roll. These contractions finished in ~80 s (Fig. S10), which provided an average power density of ~0.9 W/kg. Upon water sorption, this 25-mg free film could deform and lift a 9.5 g load to the height of 2 mm within 3 second (Fig. 3C). The work output was 7.6 J/kg and the power density was 2.5 W/kg. In addition, we found that a load of silver wires up to 260 mg attached to the film perimeter was efficiently transported along a substrate-derived water gradient (Fig. 3D, Movie S4, Fig. S11).

To probe the capability of the PEE-PPy actuator, we did a theoretical thermodynamic analysis of its water-induced expansion-contraction cycle and came up with the following two equations (see SOM for detailed analysis).

$$\frac{E \times d}{R} < \frac{(-\Delta G_{cycle} \times \rho)}{M} \quad (1)$$

$$\frac{E \times d^3}{2R^2} > f_{ad} \quad (2)$$

E, d and R are the elastic modulus, thickness and curvature of the buckled actuator, respectively. ρ and M are the density and molecular weight of water, respectively. ΔG_{cycle} is the molar Gibbs free energy change of absorbed water during one expansion-contraction cycle. f_{ad} is the adhesive force coefficient between PEE-PPy films and moist substrates. Given a certain E, R and f_{ad}, equations 1 and 2 roughly define a theoretical maximum and minimum limit on the required thickness of the actuator to perform fast locomotion. In practice, we found that the optimal thickness for PEE-PPy actuators on a moist paper was roughly 15-40 μm. Actuators thinner than 15 μm tended to stick to the moist paper, while actuators thicker than 40 μm showed significantly slower locomotion.

Since this PEE-PPy actuator could continuously extract chemical potential energy out of ambient water gradients to perform mechanical work, it should be able to drive a piezoelectric element to convert the mechanical energy into electrical energy. A 9-μm-thick piezoelectric polyvinylidene difluoride (PVDF) film was metallized, wired and insulated on both faces (Fig. 4A). A 27-μm-thick PEE-PPy actuator was attached to one face of the PVDF element. When placed on a moist substrate with the actuator facing down, the actuator bent and stretched the PVDF element repeatedly (Movie S5), generating an open-circuit voltage up to 3 V. A 10-MΩ resistor was loaded onto this generator (Fig. 4B) and the peak output reached ~1.0 V (Fig. 4D). Analysis indicated that the frequency of the alternating voltage signal was ~0.3 Hz (Fig. S12), which matched the motion frequency of the generator (Movie S5). The average power output was 5.6 nW (Fig. S13), which corresponded to a power density of 56 μW/kg for the 100-mg generator. In contrast, the same PVDF element did not move on the moist substrate and the recording showed only noise (Fig. S14), with analysis of this background noise giving an average power output of 0.015 nW (Fig. S15). The generated alternating electrical pulses by the generator were rectified using a commercial full-wave bridge rectifier, then stored in a 2.2 μF capacitor (Fig. 4C). Within 7 minutes of charging, the voltage of the capacitor was saturated to ~0.66 V (Fig. 4E). This was lower than the peak output voltage of the generator, possibly due to voltage drop across the rectifying diodes and/or current leakage of the capacitor.

In conclusion, this PEE-PPy polymer composite system features an interpenetrating network of a rigid polymer with a soft, hydrolytically sensitive polymer that can perform water-gradient-induced displacement, converting chemical potential energy in water gradients to

mechanical work. Besides mechanical vibration energy, the generator based on this powerful actuator can utilize ubiquitous low-temperature water gradients as its energy source, in contrast to state-of-the-art piezoelectric energy scavengers that solely rely on mechanical vibration energy (26). Thus, the water-gradient-driven actuator and generator demonstrated potential applications as sensors, switches and power sources for ultra-low power devices.

Supplementary Material

Refer to Web version on PubMed Central for supplementary material.

Acknowledgments

M.M. and R.L. conceived the idea and designed the experiments. M.M. and L.G. performed the experiments. M.M., L.G., D.A. and R.L. contributed materials/tools, analyzed the data, and wrote the paper. This research was supported in part by NHLBI PEN Award, Contract #HHSN268201000045C; NCI Grant CA151884; and AFIRM Award #W81XWH-08-2-0034. Experimental procedures, additional data for material characterization and device test are presented in SOM. We thank Dr. Dennis Bong for thoughtful discussion and Dr. Ning Zhang for help of preparation of figures.

References and Notes

1. Minko, S. Responsive polymer materials: design and applications. Blackwell Pub; Ames, Iowa: 2006.
2. Jager EWH, Smela E, Inganas O. Science. 2000; 290:1540. [PubMed: 11090345]
3. Osada Y, Okuzaki H, Hori H. Nature. 1992; 355:242.
4. Lendlein A, Jiang HY, Junger O, Langer R. Nature. 2005; 434:879. [PubMed: 15829960]
5. Lendlein A, Langer R. Science. 2002; 296:1673. [PubMed: 11976407]
6. Camacho-Lopez M, Finkelmann H, Palffy-Muhoray P, Shelley M. Nature Mater. 2004; 3:307. [PubMed: 15107840]
7. van Oosten CL, Bastiaansen CWM, Broer DJ. Nature Mater. 2009; 8:677. [PubMed: 19561599]
8. Yu Y, Nakano M, Ikeda T. Nature. 2003; 425:145. [PubMed: 12968169]
9. Kim J, Hanna JA, Byun M, Santangelo CD, Hayward RC. Science. 2012; 335:1201. [PubMed: 22403385]
10. Sidorenko A, Krupenkin T, Taylor A, Fratzl P, Aizenberg J. Science. 2007; 315:487. [PubMed: 17255505]
11. Beebe DJ, et al. Nature. 2000; 404:588. [PubMed: 10766238]
12. Chen GH, Hoffman AS. Nature. 1995; 373:49. [PubMed: 7800038]
13. Benns JM, Choi JS, Mahato RI, Park JS, Kim SW. Bioconjugate Chem. 2000; 11:637.
14. Caldorera-Moore ME, Liechty WB, Peppas NA. Acc Chem Res. 2011; 44:1061. [PubMed: 21932809]
15. Fratzl P, Barth FG. Nature. 2009; 462:442. [PubMed: 19940914]
16. Smela E. Adv Mater. 2003; 15:481.
17. Baughman RH. Science. 2005; 308:63. [PubMed: 15802593]
18. Okuzaki H, Kuwabara T, Kunugi T. J Polym Sci Polym Phys. 1998; 36:2237.
19. Ushiki T. Arch Histol Cytol. 2002; 65:109. [PubMed: 12164335]
20. Shibayama M, Sato M, Kimura Y, Fujiwara H, Nomura S. Polymer. 1988; 29:336.
21. Park T, Zimmerman SC. J Am Chem Soc. 2006; 128:13986. [PubMed: 17061855]
22. Ren XM, Pickup PG. J Phys Chem. 1993; 97:5356.
23. Szafran M, Degaszafran Z. J Mol Struct. 1994; 321:57.
24. Hara S, Zama T, Takashima W, Kaneto K. Polym J. 2004; 36:151.
25. Madden, JD.; Madden, PG.; Anquetil, PA.; Hunter, IW. Electroactive Polymers and Rapid Prototyping. Vol. 698. MRS; Warrendale: 2002. p. 137
26. Qin Y, Wang X, Wang ZL. Nature. 2008; 451:809. [PubMed: 18273015]

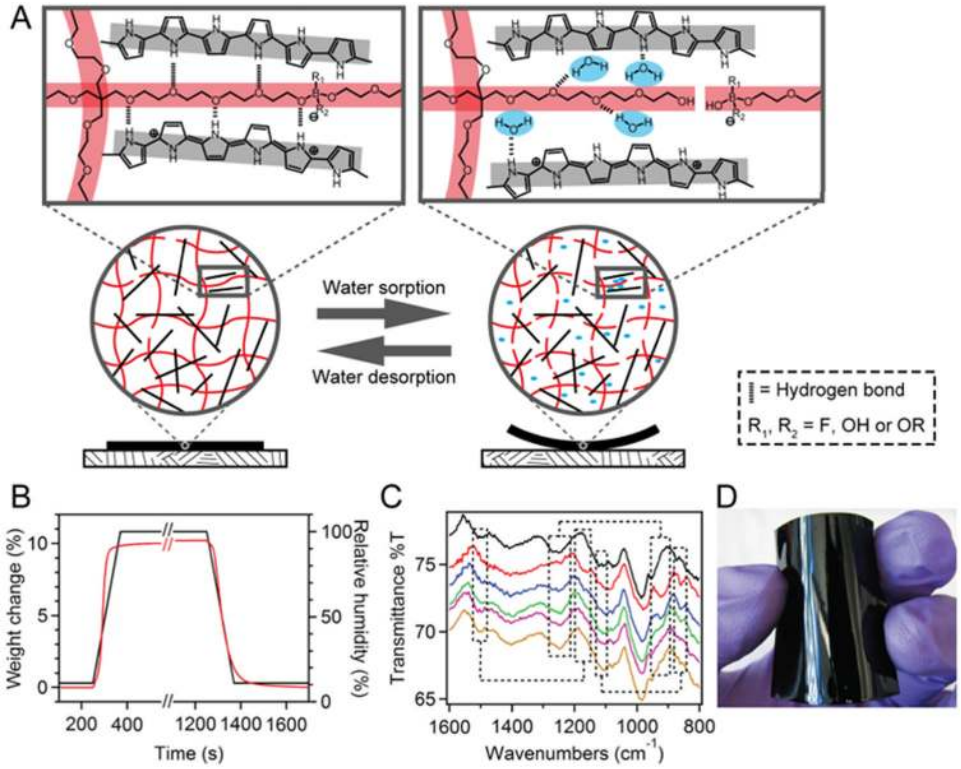

Fig.1.

Characterization of PEE-PPy composite films. (A) A PEE-PPy composite film (black) is composed of PPy polymer chains (grey lines) and PEE-borate network (red lines). The structure changes (involving hydrogen bonds and borate ester bonds) in response to water (blue dots) sorption and desorption. (B) PEE-PPy weight change (red) synchronizes air humidity change (black). (C) ATR-IR spectra showing H/D exchange between PEE-PPy film and water vapor. From top to bottom: before D_2O exposure; 0, 1, 2, 3 and 4 min after D_2O exposure. Dashed lines indicate the three pairs of shifting peaks. (D) A PEE-PPy film maintains its flexibility and mirror-like surface after six-month open storage.

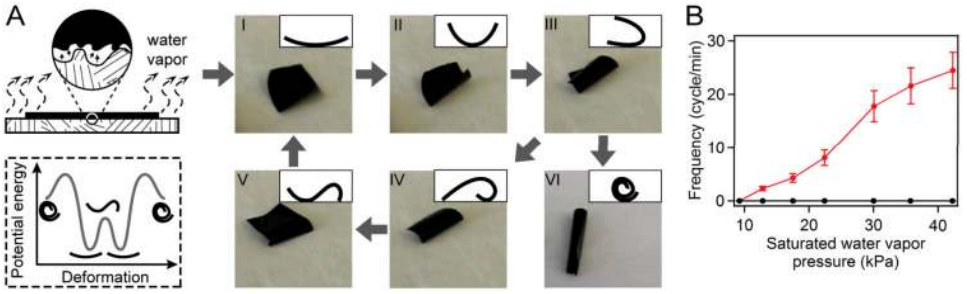

Fig. 2.

Locomotion of a PEE-PPy film on a moist substrate. (A) Representative images and sketches of the film's multi-stage locomotion, and a schematic diagram of the film's elastic potential energy. (B) Flipping frequency of PEE-PPy (red) and PPy (black) films correlated to saturated water vapor pressure at each substrate temperature (N = 5). One flipping cycle refers to a motion process starting from Stage I through Stage V and back to Stage I.

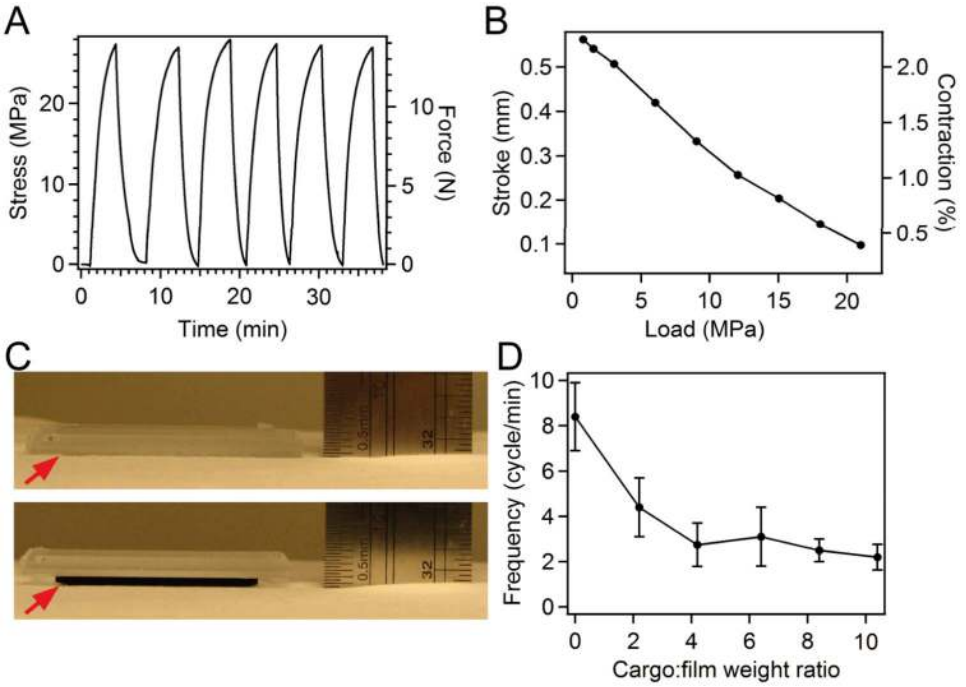

Fig. 3.

Mechanical performance of a 25-mg PEE-PPy film actuator. (A) The contractile stress and force generated in the film upon water sorption and desorption. (B) The load-dependent stroke of the actuator contraction. (C) Images of the actuator under microscopy glass slides (top image) buckling and lifting the slides up for ~2 mm (bottom image). The red arrows indicate the position of the 30-μm-thick actuator. (D) The flipping frequency of the actuator with cargo loading (N =5).

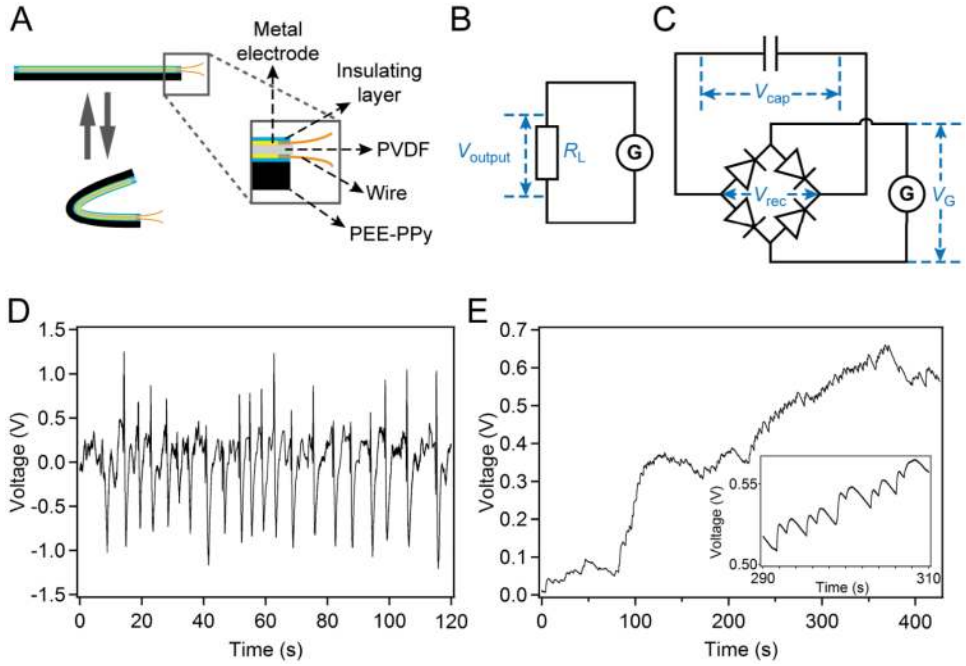

Fig. 4.

Design and performance of a water-gradient-driven generator. (A) The assembly of a piezoelectric PVDF element with a PEE-PPy actuator to form the generator. (B) The connection of the generator with a 10-MΩ resistor as load. (C) The configuration of the rectifying circuit and charge storage capacitor. (D) Generator's output voltage onto the 10-MΩ resistor. (E) Voltage across a capacitor when being charged by the generator. Insert shows a stepwise increase in the capacitor voltage accompanying each cycle of energy conversion process.